United States
Department of
Agriculture

Forest Service

**Forest
Products
Laboratory**

Research
Paper
FPL 367

September 1980

Smoldering Wave-Front Velocity in Fiberboard

Abstract

In fiberboard, the phenomena of smoldering can be visualized as decomposition resulting from the motion of a thermal wave-front through the material. The tendency to smolder is then directly proportional to the velocity of the front. Velocity measurements were made on four fiberboards and were compared to values given in the literature for several substances. Velocities ranged from zero to 4.63×10^{-2} inch per minute (11.8 cm/min). The phenomena of smoldering is also considered in terms of transport processes; a discussion of related literature and theory is provided, culminating in the wave-front propagation model.

United States
Department of
Agriculture

Forest Service

**Forest
Products
Laboratory**[1]

Research
Paper
FPL 367

Smoldering Wave-Front Velocity in Fiberboard

By
JOHN J. BRENDEN, Research Chemical Engineer
and
ERWIN L. SCHAFFER, Supervisory Research Engineer

Introduction

The history of fiberboard, also known as "insulation board," can be traced back to the year 1914. Over the years, manufacturing technology and sophistication have vastly increased to a point where, today, structural fiberboards with specially tailored properties are commonplace. Moreover, these "boards" are manufactured in large quantities for use in a broad spectrum of housing and building applications. One product of this type, sound-deadening board, is made for use in applications where sound reduction and control are desired.

In the latter part of 1973 and in 1974, reports *(4)*[2] began to appear documenting fire experiences with buildings that contained walls and partitions fabricated using sound-deadening board. The reports "indicated" that sound-deadening board had, on occasion, been ignited by a plumber during a joint-sweating operation or, in one case, by a welding torch during the installation of an air-conditioning system. In these cases, the workmen involved were apparently unaware that smoldering continued in the involved material. Flames were observed in the vicinity of the exposure from 30 minutes to several hours later.

As a result of these incidents, research was undertaken at the Forest Products Laboratory, and in the fiberboard industry, with a view toward reducing or eliminating the smoldering tendency of fiberboard products. It soon became apparent that relatively little was known about the subject of smoldering and that there was no known method for measuring the smoldering tendency of fiberboards.

An examination of available mathematical models describing the phenomena together with the development of a test method to evaluate the smoldering tendency of fiberboard was begun. Detailed comments and a review of pertinent literature are given in appendix A.

Beginning with the early work of Palmer *(8)* and at the Forest Products Laboratory by Van Kleeck and Sandberg (appendix B), a qualitative understanding of the events that constitute smoldering has evolved. It is pictured as the perpetuation of the thermal decomposition process once the process has been initiated. The distinguishing feature of the phenomena is that thermal degradation may proceed without accompanying flames or visible glowing of the affected material. The only notable characteristics may be temperature changes and changes in the weight and/or appearance of substances in the region of interest. There have been at least three attempts to develop quantitative mathematical models of the process or related effects; these are discussed more fully in appendix A.

One of the concepts that emerges from the literature review is that smoldering can be viewed much like a reaction wave moving through virgin (unreacted) material. The tendency to smolder can then be related to the velocity of this **wave:** Zero velocity corresponds to a nonsmoldering substrate. Higher velocities correspond to a greater tendency to perpetuate thermal decomposition.

It is also shown in the appendix

[1] Maintained at Madison, Wis., in cooperation with the University of Wisconsin.

[2] Italicized numbers in parentheses refer to literature cited at the end of this report.

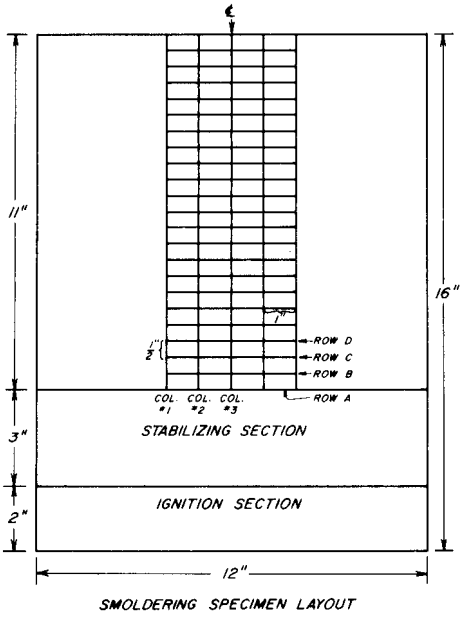

Figure 1.–Specimen with scribed grid for smoldering test.
(M 148 871)

that many factors influence the wave-front velocity, including the physical and chemical properties of the solid phase, the composition of the surrounding gaseous phase, and any relative motion between the two phases.

Experimental Work

Appendix A shows that from the early work of Palmer *(8),* and through the development of the several mathematical models *(6, 7, 10),* one of the most important parameters of interest is the propagation velocity of the smoldering wave-front; all of the proposed models yield estimates of this quantity. Thus it is possible to define the "tendency to smolder" in terms of the smolder wave propagation: materials with high velocities have a high smoldering tendency and vice versa. In the limiting case where the velocity is zero, extinguishment occurs and the material of interest can be said to have no tendency to smolder. A more detailed discussion of extinguishment limits has been given by Moussa, Toong, and Garris *(6).*

Description of Materials and Specimens

Fiberboards are made in several thicknesses and densities, and have differing ingredients in addition to cellulosic fiber. Using the material properties influencing smoldering rate as a guide, an effort was made to obtain panels of constant thickness but with a range in density as produced commercially. Descriptive information on each panel type obtained is given as follows:

Designation	Description
B-1	One-half-inch-thick sound-deadening board; bulk density: 15 pounds per cubic foot (sp. gr. 0.240); 95 percent pine with 5 percent hardwood; integral treatment of asphalt emulsion.
E-1	One-half-inch-thick sound-deadening board manufactured from aspen fibers with no integral treatment; bulk density: 15.3 pounds per cubic foot (sp. gr. 0.245).
E-2	One-half-inch-thick intermediate grade sheathing; manufactured from aspen fibers with an integral treatment of pulverized asphalt; bulk density: 20.3 pounds per cubic foot (sp. gr. 0.325).
E-3	One-half-inch-thick nail-base sheathing manufactured from aspen fibers with an integral treatment of pulverized asphalt; bulk density: 27.0 pounds per cubic foot (sp. gr. 0.433).

Specimens of 12 by 16 inches were cut from larger sheets of the fiberboards and conditioned at 80° F and 30 percent relative humidity for at least 2 weeks or until moisture equilibrium had been reached. When conditioning was completed, the specimens were scribed with the grid shown in figure 1 using a ballpoint pen. Care was taken to cause as little other disturbance as possible to the surface of the test material.

Experimental Wave-Front Velocity Measurements

Measurement of the smoldering velocity can be divided into two basic parts: first, the initiation of the smoldering wave, and second, the actual smoldering-velocity determination.

Before starting a determination, the airflow velocity into the enclosure (hood) where the test would be performed was checked and adjusted. Figure 2 shows such a measurement being made using an anemometer probe and a blank (unignited) specimen. The approach-air velocity at a point in line with the specimen centerline, in the horizontal plane of the specimen, and 2 inches upstream of the leading edge, was adjusted to be in the range of 20 to 35 feet per minute during all of the experimental work.

As shown in figure 3, two aluminum plates, 4 by 15 by 1/4 inch, were clamped around the specimen with C-clamps to prepare it for ignition. When noncombustible inserts were placed alongside the specimen between the plates to seal its sides, only the "ignition section" of the sample remained exposed upstream of the plates. Then a Bunsen burner flame (burning natural gas) was manually applied with a back-and-forth motion to the front of the ignition section until it was evenly ignited on both top and bottom surfaces. The section was allowed to burn until the flames were quenched by the metal plates. If necessary, the burner flame was reapplied until no more than 1/8 inch of unburned material remained ahead of the metal plates. When no flames had been observed for a period of 10 seconds, the plates were gently removed; the specimen was then considered to be ignited. If smoldering of the specimen could not be induced using this procedure, the material was considered to have a smoldering velocity of zero.

Once a test specimen was ignited, it was placed in a holding apparatus (clamps) as shown in figure 4. Placement was accomplished as soon as possible after ignition. The specimen was level in the clamps and its top surface was 1 foot above the hood-chamber floor. After mounting and leveling, the specimen was allowed to smolder as the induced smoldering wave-front passed through the "stabilizing zone" shown in figure 1.

The position of the smoldering combustion front was detected by embedding thermocouples in the ignited test specimen. The front was said to arrive at a point in the specimen when the temperature of that point reached 600° F. The first temperature measurements were made by placing five 24-gage, chromel-alumel thermocouples along the line in the grid (see fig. 1), separating the stabilizing section from the measuring section. This line of thermocouples was termed "row A" and is shown in place in figure 4. For convenience, the thermocouples were secured in a wire-holding device above the smoldering specimen as shown in the figure. Placement of the thermocouples was accomplished by first making a small hole at the appropriate location with an awl so the thermocouple bead fit snugly at a depth near the specimen center. The time at which each of the thermocouples in row A reached 600° F was noted.

Once the smoldering wave had passed row A, the thermocouples were gently removed from the resulting char and moved back 1/2 inch from their original locations to form a second row, row B. Again, the time at which the smoldering wave passed was noted and the thermocouples were moved back 1/2 inch (to row C). By noting the time at which the thermocouple in column 1 reached 600° F in row A and then in row B, etc., it was possible to make a table of data giving the motion of the combustion wave as measured in column 1; in the same way, data could be collected for columns 2, 3, 4, and 5. A completed data table for a typical determination is shown as table 1. For some materials, the char residue remaining after passage of the smoldering front tended to "curl over" in the direction of unburned material. In these cases, the char "curls" were gently tipped backward to avoid disturbing the moving char line. During the determination, care was taken that the specimen remained level.

The calculations involve using data like that in table 1 to determine the rate of travel of the smoldering wavefront. To do this, a "regression line" was determined for the time-distance data in each column by the method of least squares. The smoldering velocity is then the reciprocal of the slope of the best-fit line; five estimates of smoldering velocity are obtained for each specimen. In table 1, the smoldering velocities determined from the data in each of the five columns are given at the bottom of the columns. The data showed that there was a slight "acceleration" of the rate of smoldering with decomposition distance; hence, the results are based on the first five rows (rows A-E). However, the "acceleration," probably due to accumulating edge effects, amounted to only about 1 percent of the velocity values when data for the first five rows were compared to the data for all rows in many specimens. The comparison for one particular specimen is given in table 2.

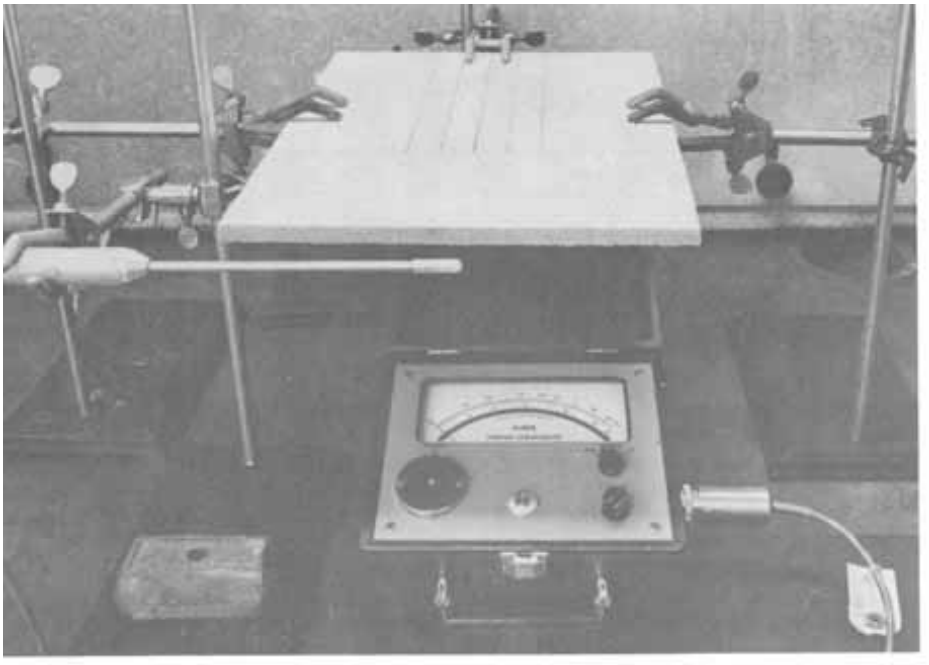

Figure P.-Level specimen with probe in place for approach-air velocity measurement.

(M 145 913-1)

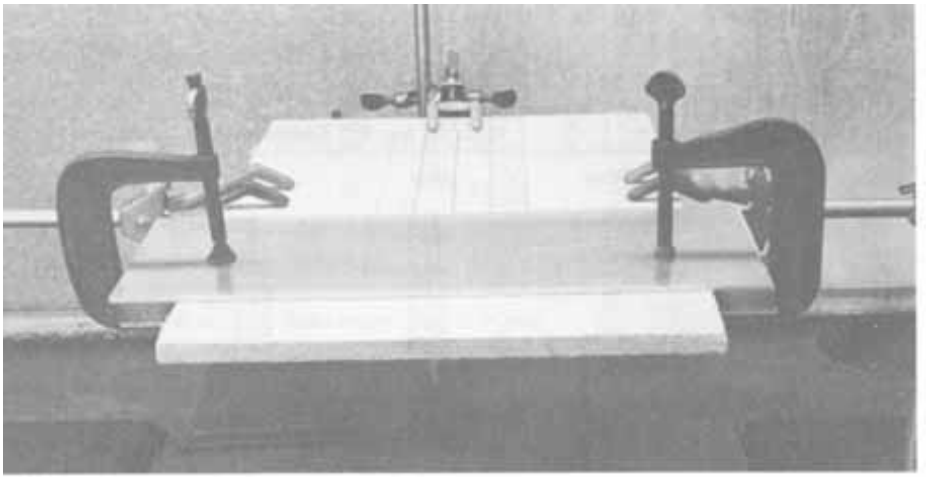

Figure 3.–Specimen with plates clamped in place just prior to ignition.

(M 145 913-2)

Results and Discussion

Materials E-2 and E-3 could not be induced to smolder using the procedure outlined previously; therefore, they have a smoldering velocity of zero. Tables 3 and 4 give results of smoldering-velocity determinations on materials B-1 and E-1. Also shown are the 90 and 95 percent confidence intervals for the smoldering velocity of individual specimens and for the in-

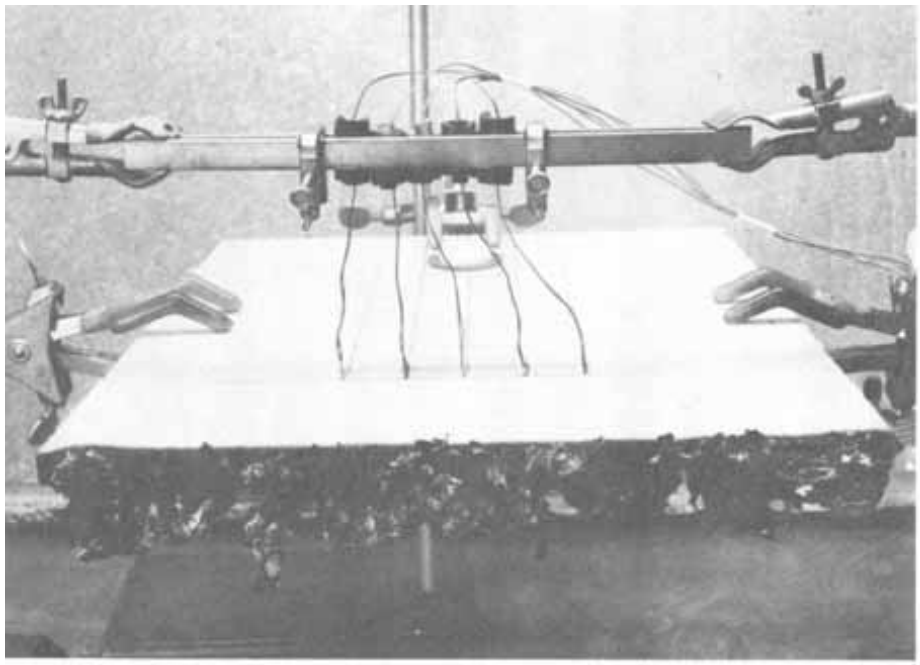

Figure 4.–Smoldering specimen with thermocouples in row A and circular level gage in front of rear clamp.
(M 145 913-6)

dividual columns of all specimens.

Tables 3 and 4 give useful information relating to the experimental method, as well as the velocity values themselves. For example, in both of the tables, the grand-mean velocity value lies within the 95 percent confidence interval of the column-mean values. In addition, there is no meaningful difference between column-means in the individual tables. Further, values of the "degree of fit," r^2, observed in processing the data, were almost always in the range of $r^2 > 0.99$. Taken together, these observations indicate that a stable, well-defined smoldering wave front with negligible "edge effects" was induced in the test specimen. The 90 and 95 percent confidence intervals for some specimen-mean velocities, however, did fall outside the like intervals for the grand-mean velocity. This is an indication of a rather high variability of smoldering tendency from specimen to specimen. Considering this variability, extreme caution should be used in comparing a single determination of one material with a single

Table 1.–Data for smoldering velocity determination[1]

Position of front (in. from start)		Time of arrival				
		Column No. 1	Column No. 2	Column No. 3	Column No. 4	Column No. 5
In.	Row	Min	Min	Min	Min	Min
0.0	(A)	5.4	7.1	6.9	7.9	5.4
.5	(B)	17.4	19.3	17.8	20.0	18.5
1.0	(C)	29.6	30.8	29.7	32.3	31.3
1.5	(D)	42.3	42.8	42.8	43.2	43.0
2.0	(E)	53.6	52.9	53.6	56.8	55.2
2.5	(F)	63.9	66.2	66.0	67.3	66.0
3.0	(G)	77.4	80.3	80.1	79.0	78.0
3.5	(H)	89.0	93.2	91.7	90.6	89.9
4.0	(I)	102.8	103.5	103.8	102.1	100.2
4.5	(J)	112.8	116.7	115.8	116.2	111.3
5.0	(K)	124.0	127.8	127.2	128.2	124.4
Slope (min/in.)		23.84	24.35	24.37	23.87	23.45
Smoldering velocity (in./min)		4.19×10^{-2}	4.11×10^{-2}	4.10×10^{-2}	4.19×10^{-2}	4.27×10^{-2}
Degree of fit (r^2)		1.000	0.999	1.000	1.000	0.999

[1] Summaries of these data also appear in tables 2 and 3.

Table 2.–Comparison of results obtained using 5 and 11 rows to calculate smoldering velocity[1]

	Column No. 1	Column No. 2	Column No. 3	Column No. 4	Column No. 5
Rows A-E					
Smoldering velocity (in./min)	4.12×10^{-2}	4.34×10^{-2}	4.22×10^{-2}	4.13×10^{-2}	4.03×10^{-2}
r^2	1.000	0.999	0.999	0.999	1.000
Rows A-K					
Smoldering velocity (in./min)	4.19×10^{-2}	4.11×10^{-2}	4.10×10^{-2}	4.19×10^{-2}	4.27×10^{-2}
r^2	1.000	0.999	1.000	1.000	0.999

[1] Rows A-E appear as determination No. 8 in table 3

determination of another material, even if the mean of the five velocity measurements (the mean of the five columns) on each specimen is used.

Several values for smoldering velocity have been reported in the literature; many of these were tabulated by Friedman *(3)* and are given in table 5. Considering the differences in test materials, densities, and other factors, the data given in table 5 agree fairly well with the determinations reported here (see, for example, fiberboard, at 27 gm/cc). With reference to the early work by Palmer *(8)* which leads to equation (1) appendix A, it is possible to estimate smoldering-velocity values using that model and his experimentally derived parameters. For example, Palmer gives $C = 4.9 \times 10^{-4}$ and $n = 0.44$ for horizontally smoldering fiberboard; if $V = 15$ centimeters/second (i.e., 30 ft/min), as in the current study, equation (1) yields a smoldering velocity, R, of 3.8 Svu, in good agreement with tables 3 and 4. Moussa, et al. *(6),* obtained smoldering rates of 1.3 centimeters/second (51.2 Svu) in air for horizontally-held cylinders having a diameter of 0.86 centimeter. The higher velocity value observed in that case might be explained on the basis of density and composition (pure a-cellulose having a density of 0.06 gm/cc was used). Data given by Rothermel *(10)* tend to be at variance, by several orders of magnitude, when compared to the values given here; this is undoubtedly due to the poor analogy between fuel beds or arrays and fiberboard products.

Table 3.–Summary of smoldering test data for material B-1

Determination No.	V_1 (Column No.1) Svu[1]	V_2 (Column No. 2) Svu[1]	V_3 (Column No. 3) Svu[1]	V_4 (Column No. 4) Svu[1]	V_5 (Column No. 5) Svu[1]	$\overline{V}$ (Mean) Svu[1]	V^{**2} (95 percent confidence) Svu[1]	V^{*2} (90 percent confidence) Svu[1]
1	4.21	3.86	3.83	4.01	3.82	3.95	4.15-3.74	4.10-3.79
2	3.94	3.99	4.10	4.01	4.59	4.13	4.46-3.80	4.38-3.87
3	4.13	4.14	4.25	4.39	4.34	4.25	4.40-4.11	4.36-4.14
4	4.92	5.09	4.60	4.38	4.43	4.68	5.07-4.30	4.98-4.39
5	4.40	4.31	4.16	4.41	4.51	4.36	4.52-4.20	4.48-4.23
6	4.67	4.51	4.37	4.37	4.52	4.49	4.64-4.33	4.61-4.37
7	4.20	4.41	4.22	4.16	4.31	4.26	4.38-4.14	4.36-4.16
8	4.12	4.34	4.22	4.13	4.03	4.17	4.31-4.02	4.28-4.06
9	3.97	3.91	4.29	4.26	4.33	4.15	4.40-3.91	4.34-3.97
10	4.46	4.51	4.47	4.60	4.51	4.51	4.58-4.44	4.56-4.46
11	4.67	4.63	4.75	4.59	4.60	4.65	4.73-4.57	4.71-4.59
12	4.49	4.37	4.33	4.43	4.28	4.38	4.48-4.28	4.46-4.30
(Mean) $\overline{V}$	4.35	4.34	4.30	4.31	4.36	4.33		
V^{**2}	4.54-4.16	4.56-4.12	4.45-4.15	4.44-4.19	4.50-4.21		4.40-4.26	
V^{*2}	4.51-4.19	4.52-4.16	4.42-4.18	4.42-4.21	4.48-4.24			4.39-4.28

[1] Svu = smoldering velocity unit; Svu = 1.0×10^{-2} in./min.
[2] V^* is the 90 pct confidence interval for $\overline{V}$ (in Svu); V^{**} is the 95 pct confidence interval for $\overline{V}$ (in Svu).

Table 4.–Summary of smoldering test data for material E-1

Determination No.	V_1 (Column No.1) Svu[1]	V_2 (Column No. 2) Svu[1]	V_3 (Column No. 3) Svu[1]	V_4 (Column No. 4) Svu[1]	V_5 (Column No. 5) Svu[1]	$\overline{V}$ (Mean) Svu[1]	V^{**2} (95 percent confidence) Svu[1]	V^{*2} (90 percent confidence) Svu[1]
1	4.38	4.78	4.85	4.32	4.45	4.56	4.86-4.26	4.79-4.33
2	5.00	4.97	4.89	4.22	4.16	4.65	5.17-4.13	5.05-4.25
3	4.85	4.68	4.39	4.38	4.37	4.53	4.81-4.26	4.74-4.33
4	4.79	5.04	5.06	5.42	4.77	5.02	5.34-4.69	5.27-4.77
5	5.09	4.91	4.96	4.52	4.87	4.87	5.13-4.61	5.07-4.67
6	4.60	4.62	4.55	4.61	4.52	4.58	4.63-4.53	4.62-4.54
7	4.42	4.82	4.69	4.46	4.58	4.59	4.80-4.39	4.75-4.44
8	4.44	4.63	4.55	4.51	4.69	4.56	4.69-4.44	4.66-4.47
9	4.46	4.60	4.65	4.55	4.70	4.59	4.71-4.48	4.68-4.50
10	4.46	4.48	4.62	4.43	4.45	4.49	4.58-4.39	4.56-4.42
11	4.62	4.57	4.66	4.52	4.58	4.59	4.66-4.52	4.64-4.54
12	4.70	4.54	4.51	4.58	4.58	4.58	4.67-4.49	4.65-4.51
(Mean) $\overline{V}$	4.65	4.72	4.70	4.54	4.56	4.63		
V^{**2}	4.80-4.50	4.84-4.61	4.83-4.57	4.73-4.35	4.68-4.44		4.69-4.58	
V^{*2}	4.77-4.53	4.81-4.63	4.80-4.59	4.70-4.39	4.66-4.46			4.68-4.58

[1] Svu = smoldering velocity unit; Svu = 1.0×10^{-2} in./min.
[2] V^* is the 90 pct confidence interval for $\overline{V}$ (in Svu); V^{**} is the 95 pct confidence interval for $\overline{V}$ (in Svu).

Table 5.–Smolder propagation rates for various materials (from a compilation by Friedman *(3)*)

Material	Rate	Rate
	cm/min	Svu[1]
Beech sawdust, 200 h	0.10	3.9
Coal, < 104 μ	0.10	3.9
Cocoa, < 40 μ	0.16	6.3
Lycopodium, < 40 μ	0.19	7.5
Fiberboard, 0.27 gm/cc	0.20	7.9
Sawdust, undried, 76-152 μ	0.24	9.5
Cigarette, between puffs	0.30	11.8
Paper roll, 0.66 cm diam., 40° C	0.30	11.8
Paper roll, 0.4 cm diam., 40° C	0.44	17.3
Cardboard, 1 cm wide, 0.076 cm thick, 60° C	0.60	23.6
Cotton, single yarn, 0.028 cm dia., 0.7 gm/cc	5.4	213
Cotton string, 0.045 cm diam., 0.22 gm/cc	10.8	425

[1] Svu = smoldering velocity unit; 1 Svu = 1.0 x 10^{-2} in./min.

Conclusions

Besides the absolute values of smoldering velocity, the experimental determinations also yield the following conclusions:

1. The rather simple proposed test method provides a means to reproducibly measure smoldering wavefront velocity in a fiberboard panel. Both nonsmoldering and smoldering tendencies can be ascertained using the technique.
2. Materials E-2 and E-3 (0.325 and 0.433 sp. gr., respectively) do not have a tendency to smolder.
3. Material E-1 (sp. gr. 0.245) has a more rapid smolder rate than material B-1 (sp. gr. 0.240).
4. Comparisons of smoldering tendency should be made using several specimens of each material being examined; comparisons on the basis of single tests should be avoided.

Preliminary data also show that the airflow velocity around the smoldering specimen has a marked effect on the phenomena involved. More definitive work on the airflow velocity influence is needed.

APPENDIX A

Previous Work Relating to Smoldering Phenomena

Among the earliest references to work in this area is the data reported by Palmer (8) who experimented with several types of dusts, and with rigid fiberboard. He found a correlation of the form:

$$R = CV^n \tag{1}$$

R = smoldering rate (cm/sec)

C, n = characteristic constants

V = air velocity past the samples (cm/sec)

to be applicable to both horizontally and vertically oriented specimens of fiberboard. Another early study was conducted at the Forest Products Laboratory by Van Kleeck and Sandberg[3] who treated a limited number of cellulosic insulation boards with boric acid and monoammonium phosphate in an attempt to retard smoldering. They achieved some success with these salts, but they did not attempt to study the chemical and physical aspects of the process itself. A condensed summary of their previously unpublished test procedure and data is given in appendix B. Most authors agree, however, that the smoldering phenomena is poorly understood *(1, 3, 4, 8).* In qualitative terms, it can be pictured as fundamentally a solid-phase reaction taking place between the degradation (pyrolysis) products of virgin material and air (oxygen). The principal degradation product involved in the reaction is char *(6, 9)*; thus some authors *(9)* explain certain anomalies in the effects of fire retardants on smoldering in plastics on the basis of char-tar formation during pyrolysis.

It is worthy of note that smoldering can occur without being accompanied by either flaming combustion or visible glowing of the affected material. In fiberboard products, McCarter *(5)* has shown that small quantities of metals strongly influence smoldering, perhaps through combination with carboxyl groups.

At least three attempts have been made to develop mathematical models of the smoldering process *(6, 7)* or related phenomena (70). Working with fabric-covered polyurethanes, Ohlemiller et al. *(7)* began with a simplified equation of continuity for a nonreactive cylinder of porous material through which pyrolysis products flow:

$$\frac{\partial \dot{m}}{\partial x} = \frac{4}{d_c \phi} d(x) P'^{\,4} \tag{2}$$

Since equation (2) was written for a nonreactive material, it does not have a "source term" for the production of the flux, $\dot{m}$.

It is interesting to note that if the following dimensionless variables are introduced:

$$\dot{m}^* \rightarrow \text{dimensionless mass flux} = \frac{\dot{m}}{k_{av} P'_{1/2}} \tag{3}$$

$$x^* \rightarrow \text{dimensionless distance} = \frac{x}{L} \tag{4}$$

equation (2) can be reduced to a dimensionless equation of gas continuity:

$$\frac{\partial m^*}{\partial x^*} = \frac{4L}{d_c \phi} \cdot \frac{k(x)}{k_{av}} \cdot \frac{P'}{P'_{1/2}} \tag{5}$$

term I term II term III term IV

---

[3] Van Kleeck, Arthur, and Carl Sandberg. 1949. Glow retardation in cellulosic insulation boards. USDA For. Serv., For. Prod. Lab. Rep. on Proj. 9000-7b. Summarized in appendix B.

[4] Symbols, names, and dimensions are given in the section on nomenclature.

In equation (5), term I is the dimensionless mass flux, term II a dimensionless geometry, and term III the dimensionless material characteristics. Term IV in equation (5) is the dimensionless pressure driving force which can be written as the "unaccomplished" pressure differential:

$$\frac{P'}{P'_{1/2}} = \frac{P_{loc} - P_o}{P_{1/2} - P_o} \tag{6}$$

where:

P_{loc} = local pressure

$P_{1/2}$ = pressure at the center of the cylinder

P_o = ambient pressure

For the same model, the gas-flow energy conservation equation is given (7) as:

$$\underbrace{\frac{\partial T_G}{\partial t}}_{\text{term I}} = \underbrace{\frac{1}{P_1 T_1}\dot{m}T\frac{\partial T}{\partial x}}_{\text{term II}} + \underbrace{\left[\frac{\lambda T}{C_{pg}}\right]\frac{\partial^2 T}{\partial x^2}}_{\text{term III}} - \underbrace{\left[\frac{h_{TV}}{\phi C_p}\right]T(T-T_s)}_{\text{term IV}} - \underbrace{\frac{4k(x)}{d_c\phi}P'T(T_{air}-T)}_{\text{term V}} \tag{7}$$

In equation (7), term I is the time variation in pyrolysis gas temperature in a space element, term II represents the heat flow by convection (motion of the pyrolysis gases), term III the conduction within the gases themselves due to their own temperature variations, term IV the heat transfer between the gas and solid phases (considered as film transfer with volumetric coefficient, h_{TV}), and term V, the heat associated with the incoming air flow.

The energy equation of the solid phase is given (7) by:

$$\underbrace{\rho_s C_{ps}\frac{\partial T_s}{\partial t} = \left[\frac{1}{(1-\phi)}\right]16\phi\ell T_s^2\left[\frac{\partial T_s}{\partial x}\right]^2 + \frac{16\phi\sigma\ell T_s^3}{3}\cdot\frac{\partial^2 T_s}{\partial x^2}}_{\text{terms I and II}} + \underbrace{\alpha I_o e^{-ax}}_{\text{term III}}$$

$$+ \underbrace{(1-\phi)\lambda_s\frac{\partial^2 T_s}{\partial x^2}}_{\text{term IV}} + \underbrace{h_{TV}(T_G-T_s)}_{\text{term V}} \tag{8}$$

in which terms I and II are the internal radiative energy transport in the porous solid as approximated by conduction, term III is the absorbed radiant flux, term IV is the energy transport by conduction in the solid phase, and term V represents heat flux per unit volume (transferred across a film) from warm pyrolysis gases to the solid phase. If the following dimensionless variables are defined:

$$x^* = \alpha x \rightarrow \text{dimensionless distance} \tag{9}$$

$$t^* = \frac{\lambda t}{\rho_s C_{ps}\ell^2} \rightarrow \text{dimensionless time} \tag{10}$$

$$T_s^* = \frac{T_s}{T_{s2}} \rightarrow \text{dimensionless solid temperature} \tag{11}$$

$$T_G^* = \frac{T_G}{T_{G2}} \rightarrow \text{dimensionless gas temperature} \tag{12}$$

$$\Delta T^* = \frac{T_G - T_s}{(T_G - T_s)_2} \text{ dimensionless temperature driving force} \tag{13}$$

equation (8) can be reduced to the form:

$$\frac{\partial T_s^*}{\partial t^*} = C_1 N_1 T_s^{*2} \left[\frac{\partial T_s^*}{\partial x^*}\right]^2 + C_2 N_1 T_s^{*3} \left[\frac{\partial T_s^*}{\partial x^*}\right] + N_2 e^{-x^*} + N_3 \frac{\partial^2 T_s}{\partial x^{*2}} + N_4 \Delta T^* \tag{14}$$

where C_1, and C_2 are dimensionless coefficients and the N_1 are dimensionless heat flow numbers. The physical significance of the C_1 and N_1 can be interpreted as follows:

$$C_1 = \frac{16\phi}{1-\phi} \rightarrow \text{dimensionless porosity coefficient} \tag{15}$$

$$C_2 = \frac{16\phi}{3} \rightarrow \text{dimensionless porosity coefficient} \tag{16}$$

$$N_1 = \frac{\sigma \ell^3 T_{s2}^3 \alpha^2}{\lambda} \text{ ratio} \rightarrow \frac{\text{heat transfer by radiation}}{\text{heat transfer by conduction}} \tag{17}$$

$$N_2 = \frac{\alpha I_o \ell^2}{T_{s_2} \lambda} \text{ ratio} \rightarrow \frac{\text{radiation through "film" in solid}}{\text{heat transfer by conduction}} \tag{18}$$

$$N_3 = (1-\Phi)\ell^2 \alpha^2 \text{ approx} \rightarrow \text{resistance to heat transfer due to "optical film" around voids} \tag{19}$$

$$N_4 = \frac{h_{TV} \ell^2 (T_G - T_s)_2}{\lambda T_{s2}} \text{ ratio} \rightarrow \frac{\text{convective heat transfer in voids}}{\text{conductive heat transfer in material surrounding voids}} \tag{20}$$

thus equations (5), (7), and (14) show how material and energy conservation equations can be used in model development. It should be noted, however, that several simplifying assumptions have been made and that these equations contain no source terms from the chemical kinetics. One approach to gain further insight into the smoldering phenomena should be to solve the equations, after addition of kinetic (source) terms, through the use of transformed initial and boundary conditions. For completeness, the equation of gaseous momentum might also be included.

Moussa, Toong, and Garris *(6)* developed a model to describe smoldering in cellulosic materials by considering that the smoldering takes place in two distinct zones separated by an interface. In this model, pyrolysis is represented by two first order Arrhenius reactions, taking place concurrently, leading to the production of char and volatiles, respectively. Assumptions are that heat transfer is by solid phase conduction with local equilibrium between gas and solid phases. Additional assumptions are that the system has uniform, time invariant thermal conductivity ??? and equal specific heats for virgin cellulose, char, and volatiles. Using these assumptions, the authors solve the equations of virgin material continuity, char continuity, volatile continuity, and energy conservation with numerical integration. The equations are:

Virgin material continuity:

$$V = \frac{d\rho_u}{dx} = -\rho_u (k_c + k_g) \tag{21}$$

Char continuity:

$$V \frac{d\rho_c}{dx} = \rho_u k_c \tag{22}$$

Volatile continuity:

$$\frac{d(\rho_g v_g)}{dx} = \rho_u k_g \tag{23}$$

Conservation of energy:

$$\rho_\infty C V \frac{dT}{dx} = \lambda \frac{d^2T}{dx^2} + \rho_u (H_c k_c + H_g k_g) \tag{24}$$

with the specific reaction rates given in the form:

$$k_{c,g} = F_{c,g} \exp\left(-\frac{E_{c,g}}{R_G T}\right) \tag{25}$$

Using the more exact transport equations (21) to (24) leads to eigenvalue problems which have exact numerical solutions; approximate closed form solutions are given *(6)* for the case where $H_c = H_g \cong 0$ which leads to:

$$V = \left\{ \frac{\lambda}{\rho_\infty C} \cdot \frac{F_c}{\ell n \Omega} \left[Ei\left(-\frac{E_c}{R_G T_s}\right) + \frac{F_g}{F_c} Ei\left(-\frac{E_g}{R_G T_s}\right) - Ei\left(-\frac{E_c}{R_G T_\infty}\right) - \frac{F_g}{F_c} Ei\left(\frac{E_g}{R_G T_\infty}\right) \right] \right\}^{1/2} ; Ei(x) = \int_{-x}^{\infty} \frac{e^{-\phi} d\phi}{\phi} \tag{26}$$

in which Ei (x) is the exponential integral function. Kinetic and stoichiometric considerations also lead to the formulation of the ratio ξ, given by:

$$\xi = \frac{F_C P_{O_2,\infty}^{1/2} \exp\left(-\frac{E}{R_G T_s}\right)}{2.2 \times 10^{-5} \sqrt{T_m}\, x_{o_2,\infty}/\phi\delta} \tag{27}$$

which is the ratio of reaction times to diffusion times for the oxygen from air. It can be seen that for $\xi >> 1$ the reactions are diffusion limited while for $\xi << 1$ the reactions are kinetic limited. The authors *(6)* made measurements on cylinders of cellulose (0.86 cm diameter) mounted horizontally in quiescent oxygen/nitrogen environments of varying oxygen pressures and compositions; agreement between theory and experiment was in the range of 50 to 100 percent which is considered adequate for this type of study.

Still another model of the smoldering process can be derived by considering the work of Rothermel *(10).* He worked with advancing fire fronts in homogeneous fuel beds, and with more simplified relations containing heat fluxes, as contrasted to the generalized field equations given previously. Starting with the rate of fire spread in a homogeneous bed of fuel as given by:

$$R_s = \frac{I_{xig} + \int_{-\infty}^{0} \left(\frac{\partial I_Z}{\partial Z} \right) Z_c \, dx}{\rho_{be} Q_{ig}} \tag{28}$$

it is possible to refine the model to account for the fuel bed characteristics and simplified reaction kinetics. Qualitatively, equation (28) pictures the rate of spread, R_s, as the quotient of the driving forces (given in the numerator) reduced by the resistances (given in the denominator).

Refinements to equation (28) include designating the numerator as the "propagating flux":

$$I_p = I_{xig} + \int_{-\infty}^{0} \left(\frac{\partial I_Z}{\partial Z} \right) Z_c \, dx \tag{29}$$

and defining a quantity:

$$I_R = \frac{dw}{dt} \, h \tag{30}$$

where I_R is the "reaction intensity" or rate of heat release per unit area of the combustion front. It is then possible to relate I_p to I_R. Estimates of the physical properties of the fuel bed and the bed geometry enter into calculations of the model parameters.

It is evident from the literature reviewed that many parameters can influence the velocity of a smoldering wave-front in cellulosic materials. Material properties affecting the velocity are:

ρ_u: density *(6, 7, 10)*

d_c: geometry *(7)*

C_1, C_2: porosity or

k(x): permeability *(7),* thermal diffusibility *(6),* metallic ions present (5)

ρ_c/ρ_u: char density/virgin density *(6)*

F, E: kinetic parameters of the pyrolysis reactions

Functions { } containing these variables could be used to describe the smoldering rate in a form similar to:

$$R \propto \frac{\{k(x)\}\{F\}\{C_1, C_2\}}{\{\rho_u\}\{\rho_c/\rho_u\}\{d_c\}\{E\}} \tag{31}$$

Ambient conditions also have a profound influence. These include:
V: rate of air flow past the sample *(8),* oxygen availability (composition of the ambient atmosphere) *(6),* absolute humidity, and others.

Ideally, a test method would yield information about how most of these variables affect the propagation of a smoldering wave in the material under consideration.

Nomenclature

Symbol	Name	Units
C_p	Heat capacity	Btu(lb)$^{-1}$(°R)$^{-1}$
d_c	Diameter of hypothetical cylinder	Ft
E	Arrhenius activation energy (c = char, g = gas)	(Btu)(mole)$^{-1}$
F	Arrhenius frequency factor (c = char, g = gas)	(Min)$^{-1}$
H	Heat of reaction (c = char, g = gas)	(Btu)(lb)$^{-1}$
h_{TV}	Volumetric heat transfer film coefficient	(Btu)(ft^3)$^{-1}$(min)$^{-1}$(°F)$^{-1}$
h	Heat content of fuel	(Btu)(lb)$^{-1}$
I_o	Integration constant (Beer's Law)	(Btu)(ft^2)$^{-1}$(min)$^{-1}$
I_Z	Heat flux in vertical direction (Z-direction)	(Btu)(min)$^{-1}$(ft^2)$^{-1}$
I_p	Propagating heat flux (eq. (29))	(Btu)(min)$^{-1}$(ft^2)$^{-1}$
I_R	Reaction intensity (eq. (30))	(Btu)(min)$^{-1}$(ft^2)$^{-1}$
I_{xig}	Heat flux in X-direction absorbed by unit volume	(Btu)(min)$^{-1}$(ft^2)$^{-1}$
k	Specific rate of pyrolysis reactions (c = char, g = gas)	(Min)$^{-1}$
k(x)	Permeability in the X-direction	(Lb mass)(ft^2)$^{-1}$(min)$^{-1}$ (P')$^{-1}$
k_{av}	Average permeability	Same as k(x)
L,ℓ	Characteristic length, cell length	Ft
$\dot{m}$	Mass flux	(Lb mass)(ft^2)$^{-1}$(min)$^{-1}$
P′	Pressure gradient	(Lb force)(ft^2)$^{-1}$(ft)$^{-1}$
$P'_{1/2}$	P' at the cylinder center	Same as P′
P_{o_2}	Partial pressure of oxygen	Cm of Hg
Q_{ig}	"Heat of pre-ignition": heat required to bring unit weight of fuel to ignition	(Btu)(lb)$^{-1}$
R	Smoldering rate (smoldering velocity)	(Cm)(sec)$^{-1}$
R_G	Gas constant	(Btu)(mole)$^{-1}$(°R)$^{-1}$
R_s	Quasi-steady rate of spread in fuel bed	(Ft)(min)$^{-1}$
Svu	Smoldering velocity unit	1 x 10^{-2}(in.)(min)$^{-1}$
t	Time	Min
T	Temperature	°R or °F
T_∞	Temperature far away from reaction zone	°F

Symbol	Name	Units
T_{s2}	Temperature at midpoint-solid	°F
T_{g2}	Temperature at midpoint-gas	°F
V	Pyrolysis wave velocity	$(Ft)(min)^{-1}$
v_g	Gas flow velocity	$(Ft)(min)^{-1}$
W	Weight of fuel per unit area of fuel bed	$(Lb)(ft^2)^{-1}$
$\frac{dw}{dt}$	Mass loss rate per unit of fire front	$(Lb)(ft^2)^{-1}(min)^{-1}$
x	Distance in the X-direction	Ft
$X_{o_2,\infty}$	Mole fraction of oxygen at a long distance from the reaction zone	Dimensionless
Z	Depth of fuel bed	Ft
α	Extinction coefficient	$(Ft)^{-1}$
δ	Thickness of film boundary	Ft
σ	Stefan-Boltzman constant (radiation)	$(Btu)(min)^{-1}(ft^2)^{-1}(°R)^{-4}$
Φ	Stoichiometric ratio	Dimensionless
λ	Thermal conductivity	$(Btu)(min)^{-1}(ft^2)^{-1}(°R)^{-1}(ft)$
ρ	Density (u = virgin, unpyrolyzed) (c = char) ?? ? = far upstream) (be = effective bulk density of fuel–eq. (28))	$(Lb)(ft^3)^{-1}$
Ω	Ratio of virgin material density at interface to virgin material density at $X \rightarrow \infty$	Dimensionless
ϕ	Functional parameter (eq. (26))	Dimensionless

APPENDIX B

Summary of Unpublished Forest Products Laboratory Report

Van Kleeck, A., and C. Sandberg (1949). Glow Retardation in Cellulosic Insulation Boards.

Fire Retardant Treatments

Van Kleeck and Sandberg had treated fiberboards of about 16.5 pounds per cubic foot density to solutions of varying concentrations of monoammonium phosphate and boric acid chemical. Retentions of chemical ranged from 2.6 to 24.7 percent of weight (based upon the oven-dry weight of untreated boards). Specific retention levels were 2.95, 12.9, 19.0, and 20.8 percent for monoammonium phosphate and 2.6, 4.35, 4.60, 9.65, and 24.7 percent for boric acid. After being dried at 105° C for 24 hours and cooled, 5 x 5 x 1/2 specimens were subjected to ignition at the center of the surface by alcohol in a cup (fig. B-l) and weighed during the smoldering period (fig. B-2).

Table B-l illustrates the number of specimens which continued to smolder to varying final degrees of destruction. It was observed in this study that monoammonium phosphate treatment levels above 17 percent did not halt glowing, but did permit it to proceed at a very slow rate (about halved). Where glowing occurred in boric acid-treated specimens, it appeared to occur at a uniform rate independent of concentration. When the percentage of chemical was such that the rate of glow was substantially reduced, it was also noted that glowing usually ceased before the entire specimen was converted to char. The study had several conclusions:

(1) Boric acid is superior to monoammonium phosphate in its effect on glowing. The minimum effective concentration of boric acid was about one-quarter that of ammonium phosphate.

On the basis of this test method, glow is effectively reduced in fiberboards containing a minimum of 4.5 percent boric acid by weight, or a minimum of 19 percent by weight of monoammonium phosphate.

(2) The amount of chemical required to retard glowing in fiberboard is considerably greater than that in wood and is attributable to the porous structure of fiberboard which enhances oxygen diffusion to the glowing front.

Figure B-1.–Apparatus for supporting test specimen and alcohol cup. Specimen to be supported on top wire strand. (M 77876 F)

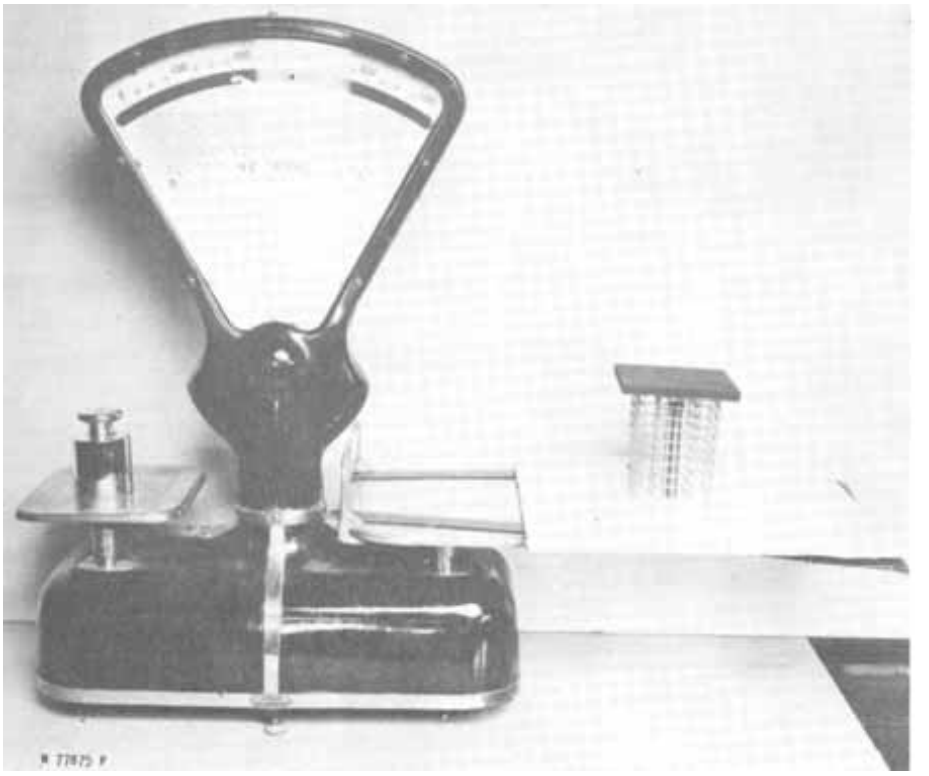

Figure B-2.–Apparatus for testing glow performance of insulation boards, showing test specimen in position. (M 77875 F)

Table B-1.—Summary of test results of glow performance of insulation board specimens

Dry chemical within specimens	Destruction of specimens by glow[1]					
	Supported on top wire strand			Supported on wire points		
	Complete	Partial	None	Complete	Partial	None
Percent[2]	No. of specimens	No. of specimens	No. of specimens	No. of specimens	No. of specimens	No. of specimens
			Monoammonium phosphate-treated specimens			
2.95	7	1				
12.9	6					
16.8	2	1				
19.0					1	3
20.8					1	3
			Boric acid-treated specimens			
2.60	2	1		2		
4.35				1	3	
4.60			2		2	
9.65			2		1	3
24.7			2			3
			Untreated specimens			
None	5			5		

[1] The destruction of specimens by glow is designated as "complete" when the specimen was reduced to a charred residue, evidenced both by weight and appearance; as "partial" when portions of the specimen remained unattacked; as "none" when glowing was not visible and the loss in weight after flaming ceased was less than 2 grams.

[2] Based on ovendry weight of specimen. Each value is the average of 5 transverse distribution determinations made on one specimen of the lot.

Literature Cited

1. Amy, L.
   1963. Smoldering fires and wood-based and wood-derived materials. Conference on wood technology. Food and Agric. Organ. of the U.N., Working Party on Fire Test Methods for Wood-Base Mater., For. Prod. Lab. Sept.

2. Bird, R. B., W. E. Stewart, and E. N. Lightfoot.
   1960. Transport phenomena. John Wiley and Sons Inc., New York, N.Y.

3. Friedman, R.
   1976. Ignition and burning of solids. Symp. on Fire Stand. and Safety, Natl. Bur. of Stand., Washington, D.C. Apr.

4. LaCosse, R. A.
   1976. Insulation board industry and sound-deadening board. Fire J. 70(3). May.

5. McCarter, R. J.
   1978. Smoldering combustion of wood fibers: cause and prevention. J. Fire and Flammability 9:119-126. Jan.

6. Moussa, N. A., T. Y. Toong, and C. A. Garris.
   1976. Mechanism of smoldering of cellulosic materials. Int. Symp. on Combust. (16th), Cambridge, Mass., p. 1447-1457. Aug.

7. Ohlemiller, T. J., F. E. Rogers, A. Kurtz, J. Bellan, and M. Summerfield.
   1976. Modeling the generation of toxic gases by the smoldering combustion of polyurethanes. Two year summary report to the Natl. Bur. of Stand. (grant 4-9026). Guggenheim Lab., Princeton Univ., Princeton, N.J. July.

8. Palmer, K. N.
   1957. Smoldering combustion in dusts and fibrous materials. Combust. and Flame 1(2):129-154. June.

9. Rogers, F. E., T. J. Ohlemiller, A. Kurtz, and M. Summerfield.
   1978. Studies of the smoldering combustion of flexible polyurethane cushioning materials. J. Fire and Flammability 9:5-11. Jan.

10. Rothermel, R. C.
    1972. A mathematical model for predicting firespread in wildland fuels. USDA For. Serv. Res. Pap. INT-115.

2.5-17-9/80

☆ U.S. GOVERNMENT PRINTING OFFICE: 1960-651-111/14